



# Molecular Modelling of Selected Combustion By-Products from the Thermal Degradation of *Croton megalocarpus* Biodiesel

Bornes C. Mosonik<sup>1,2</sup>, Silas M. Ngari<sup>1</sup>, Joshua K. Kibet<sup>1\*</sup>

<sup>1</sup>Department of Chemistry, Egerton University, Egerton, Kenya

<sup>2</sup>Department of Education Sciences, Kabarak, University, Private Bag, Kabarak, Kenya

Email: \*jkibet@egerton.ac.ke

**How to cite this paper:** Mosonik, B.C., Ngari, S.M. and Kibet, J.K. (2019) Molecular Modelling of Selected Combustion By-Products from the Thermal Degradation of *Croton megalocarpus* Biodiesel. *Open Access Library Journal*, 6: e5840.  
<https://doi.org/10.4236/oalib.1105840>

**Received:** October 8, 2019

**Accepted:** October 27, 2019

**Published:** October 30, 2019

Copyright © 2019 by author(s) and Open Access Library Inc.

This work is licensed under the Creative Commons Attribution International License (CC BY 4.0).

<http://creativecommons.org/licenses/by/4.0/>



Open Access

## Abstract

Computational models are very important in understanding the nature of interactions in chemical systems from which important geometry parameters for various organic compounds can be extracted. This study explores computationally the geometry parameters of selected volatile organic compounds from the co-pyrolysis of *Croton megalocarpus* biodiesel blend using the Density functional theory (DFT) in conjunction with B3LYP correlation function at 6 - 31 G basis set. Gaussian '16 computational and Chemissian version 4.43 computational codes were used to generate electron density maps, band gap energies and frontier molecular orbitals. Frontier orbitals are central in estimating the reactive nature of a given molecular compound. The results indicated that the thermal degradation of selected molecular products from the co-pyrolysis of *Croton megalocarpus* biodiesel blends proceeds via high energy barriers between +400 and -1250 kJ/mol. Fundamentally the highest occupied and the lowest occupied molecular orbitals (MOs) are critical in determining the reactivity of a molecule. Moreover, the HOMO-LUMO band gap energies of 4-(2,4-dimethylcyclohexyl)-2-butanone, 3,4-dimethyl-3-cyclohexene-1-carbaldehyde, 5-(3-phenylpropanoyl)dihydro-2(3H)-furanone, and isopropenyl-4-methyl-1,2-cyclohexanediol were 0.674 eV, 3.918 eV, 3.393 eV, and 1.588 eV, respectively.

## Subject Areas

Chemical Engineering & Technology

## Keywords

Optimization, Band Gap, Density Maps, Mechanisms

## 1. Introduction

Transport fuel emissions from fossil fuels have compromised air quality, affected human health for decades, and caused numerous health miseries [1]. Consequently, biomass fuels have gained enormous attention lately because they are promising renewable energy resources. These fuels have proven to reduce greenhouse gas emissions and other environmental pollutants. From recent studies carried out by [2], it is evident that the ratio of biodiesel to fossil diesel yields better combustion results which decrease the yield of toxic pollutant emissions. Biodiesel emissions have been known to be free from harmful aromatic compounds as opposed to commercial diesel [3]. This is beneficial in the combustion efficiency of biodiesel which has been noted to suffer from low oxidation ability, increased acidity and corrosion problems [4]. Environmentally persistent pollutants are considered stable and spend long lifetimes in the environment. Understanding the reactivity and stability of these pollutants is of the essence to public health practitioners and health policy authorities. One of the key factors controlling the physical properties of substances is the band gap energy, which forms the primary focus of this study. Furthermore, bond dissociation energies of these compounds are another determinant in the interpretation of the reactivity and stability of molecular compounds.

The complicated structural composition of biomass materials makes it difficult to link formation of organic pollutants to exact chemical reactions but with the use of model compounds it is possible to understand the structural entity of biomass components of significant importance in the transport industry and environmental health [5]. Hitherto, the world today is witnessing serious concerns regarding the depletion of petroleum reserves and environmental degradations because of hazardous emissions resulting to severe health consequences [6]. Biodiesel has received significant attention as an environmental friendly fuel chiefly composed of fatty acids, methyl esters derived from renewable feedstock, perceived as potential substitutes to petro-diesel for engine operations [7].

The thermal decomposition of fuels leads to the generation of smaller fragments of decomposition of biodiesel blends such as transient radicals and stable species which result in the evolution of CO<sub>2</sub> (decarboxylation reaction), olefins, water, aldehydes, ketones, and small alkanes such as methane, ethane and propane [8] [9]. Radicals formed from the thermal degradation events have generally been referred to as environmentally persistent free radicals (EPFRs) and represent a class of reactive species that have prolonged lifetime even under ambient environmental conditions [9]. Radical stabilities and reactivity can be explored by the use of computational techniques as opposed to experimental methods due to their very short half-lives. A research carried out by Kibet and co-workers (2018) has shown that some of the radicals generated by the thermal decomposition of biodiesel blends have long half-life  $\approx$  431 days. This research output shades more light on the existence of environmentally persistent free radicals (EPRs) in the environment originating from combustion events. This

study focuses on examining the physical properties of some selected volatile organic emissions from the co-pyrolysis of biodiesel blends with inclination to electronic properties.

Computational chemistry provides understanding into the molecular properties of a compound that would not otherwise be easy to determine experimentally. Additionally, computational methods are economical in terms of cost and time. This study investigates in detail the electron density maps, molecular orbitals, band gap energies and geometry optimization of selected combustion by-products of *Croton megalocarpus* bio-oil;

4-(2,4-dimethylcyclohexyl)-2-butanone,

3,4-dimethyl-3-cyclohexene-1-carbaldehyde,

5-(3-phenylpropanoyl)dihydro-2-(3H)-furanone and

isopropenyl-4-methyl-1,2-cyclohexanediol. The electron density contour maps generated was used to examine the nucleophilicity of the selected volatile organic compounds in order to gain more insight on how they interact with biological structures to cause toxicity and cellular impairment in respiratory systems. The optimization process for various pathways for the

5-(3-phenylpropanoyl)dihydro-2(3H)-furanone and intermediate free radicals was probed. Moreover, the thermochemistry and molecular models for the various mechanistic pathways for radical formation and their conversion to free molecules were proposed.

## 2. Methodology

### Density Functional Theory (DFT) Calculations

DFT calculations were performed by use of Gaussian '16 computational software [10]. Geometry parameters such as compound energetics and bond energies were calculated at the ground state geometries employing B3LYP level of theory with 6-31G basis sets. To develop molecular orbital energy-level diagrams, electronic density contour maps and the determination of the band gap energy for selected molecules, Gaussian 16 software outputs were interfaced with Chemisian version 4.43 [11]. All computational calculations were conducted at 298.15 K and 1 atmosphere. To compute the energy change for formation of a compound or a free radical from its components, the following thermodynamic equation (Equation (1)) was used [12].

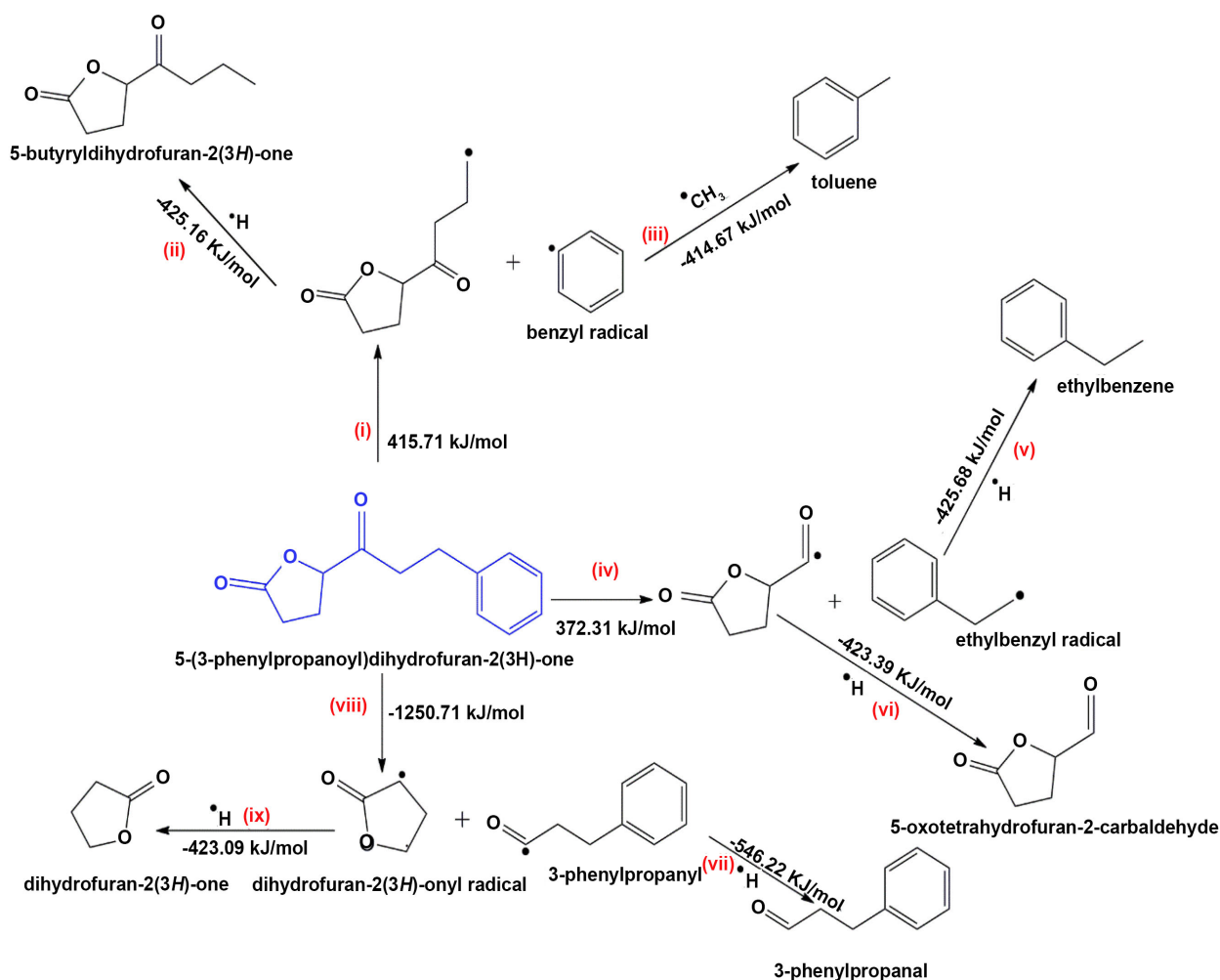
$$\Delta_r H^0 = \sum (\varepsilon_0 - H_{corr})_{\text{products}} - \sum (\varepsilon_0 - H_{corr})_{\text{Reactants}} \quad (1)$$

where,  $\Delta_r H^0$  is change in enthalpy of the reaction,  $H_{corr}$  is correction to the thermal enthalpy and  $\varepsilon_0$  is the sum of electronic and thermal enthalpies

## 3. Results and Discussion

### 3.1. Molecular Geometries of Major Molecular Emissions

Geometry parameters such as bond lengths and bond angles have a significant influence on the strength of the bonds of molecular structures. The structures of selected model components are presented in **Scheme 1**, *vide infra*. The



**Scheme 1.** Proposed mechanistic pathways for the thermal degradation of 5-(3-phenylpropanoyl) dihydro-2-(3H)-furanone.

optimization process presented below in **Figures 1-4** show steps towards achieving an optimized Structure for 4-(2,4-Dimethylcyclohexyl)-2-butanone, 3,4-Dimethyl-3-cyclohexene-1-carbaldehyde, 5-(3-phenylpropanoyl) dihydro-2(3H)-furanone and isopropenyl-4-methyl-1,2-cyclohexanediol. This offers interesting quantum mechanics results that cannot easily be accomplished by experimental methods.

The optimization of 3,4-dimethyl-3-cyclohexene-1-carbaldehyde proceeds 31 steps to attain a structure of zero energy (global minimum structure).

Interestingly, 5-(3-phenylpropanoyl) dihydro-2(3H)-furanone (**Figure 2**) required 91 steps to attain a global minima structure. This is attributed to its large molecular weight of 218.09 g/mol. The scission of C5-C6 (cf. **Figure 3**) bond in 5-(3-Phenylpropanoyl) dihydro-2(3H)-furanone proceeds with a bond dissociation energy of 372.31 kJ/mol. This was one of the thermodynamically feasible pathways (**Scheme 1**, route (i)) because it proceeds with lower energy compared to the rest of channels. The scission of C4, C5 and C7, C8 proceed with energy barriers of -1250.75 and 415.71 kJ/mol, respectively.

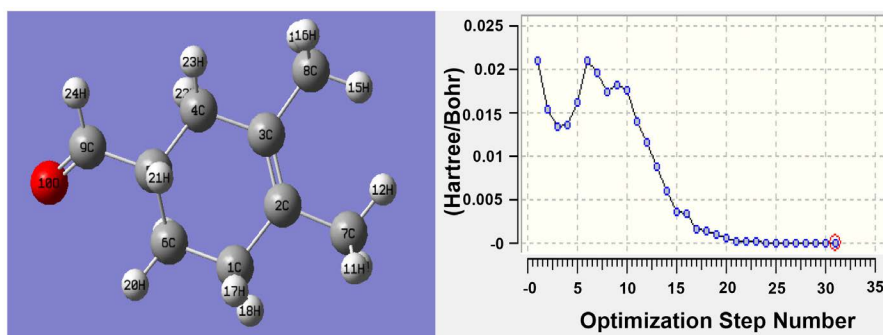


**Figure 1.** Optimized structure of 3,4-dimethyl-3-cyclohexene-1-carbaldehyde and a plot showing its optimization steps (the red circle is the optimization level).

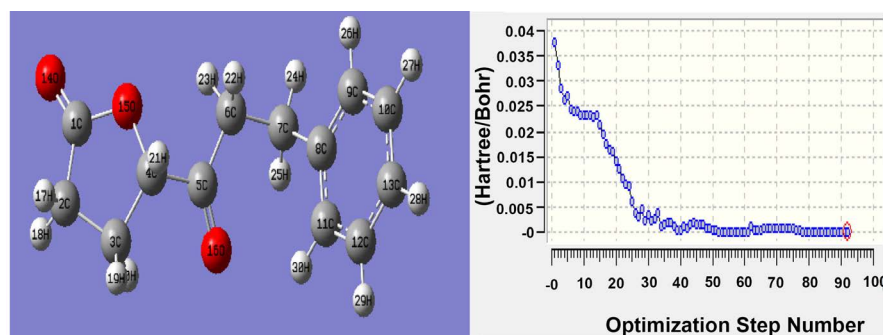


**Figure 2.** Optimized structure of 5-(3-phenylpropanoyl) dihydro-2-(3H)-furanone and a plot showing its optimization steps (the red circle is the optimization level).

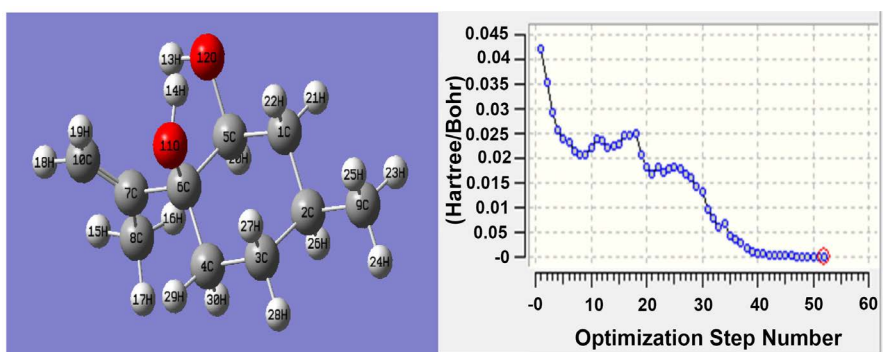


**Figure 3.** Optimized structure of isopropenyl-4-methyl-1,2-cyclohexanediol and a plot showing its optimization steps (the red circle is the optimization level).

On the other hand, isopropenyl-4-methyl-1,2-cyclohexanediol attained the global minima structure with 51 optimization steps.

4-(2,4-Dimethylcyclohexyl)-2-butanone required fewer optimization steps (36) to attain a structure of minimum energy while the scission of C10, C11 bond occurs with a bond dissociation energy of 494.24 kJ/mol. Clearly, 3,4-dimethyl-3-cyclohexene-1-carbaldehyde, takes the shortest computing time in comparison to 4-(2,4-Dimethylcyclohexyl)-2-butanone, isopropenyl-4-methyl-1,2-cyclohexanediol, and 5-(3-phenylpropanoyl) dihydro-2-(3H)-furanone, respectively.

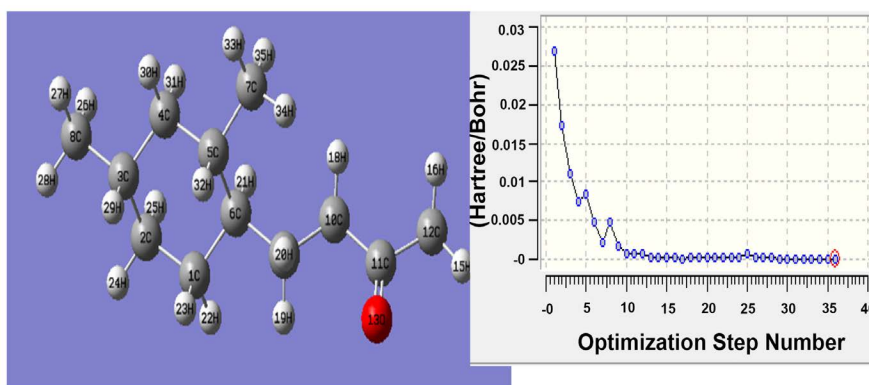


**Figure 4.** Optimized structure of 4-(2,4-dimethylcyclohexyl)-2-butanone and a plot showing its optimization steps (the red circle is the optimization level).

Fundamentally, an optimized structure of a compound or molecule is obtained after a stationary point has been during the optimization steps. At this point, the predicted change in energy is limited to zero and levels off as observed in **Figures 1-4**. Other parameters that show that optimization of a molecule is complete is the absence of imaginary vibrational frequencies in the output file of the computational platform. In the absence of negative or imaginary frequencies the structure are believed to have reached a global minima and therefore fully optimized. Remarkably, all the structures reported in this work are fully optimized based on the aforesaid arguments.

### 3.2. Frontier Molecular Orbitals and Electron Density Maps

Conventionally, frontier orbitals are the highest occupied molecular orbitals (HOMO) and the lowest unoccupied molecular orbitals (LUMO). The molecular orbitals and electron density maps are of great significance in understanding the reactivity of molecular species. The HOMO and LUMO orbitals are orbitals that are lie closer in energy of any pair of orbitals given any two molecules which tend to interact more strongly [13]. The HOMO-LUMO band-gap energies for the selected volatile organic compounds considered in this study are shown in **Table 1**. The reactivity index (HOMO-LUMO gap) of the compounds with small difference implies high reactivity and a large difference implies low reactivity in reactions, therefore as the energy gap between the HOMO and LUMO becomes smaller the rate of reaction is enhanced.

4-(2,4-dimethylcyclohexyl)-2-butanone has the smallest HOMO-LUMO energy gap (0.674 eV) and therefore considered more reactive compared to 3,4-Dimethyl-3-cyclohexene-1-carbaldehyde with a larger band gap of 3.918 eV. 5-(3-phenylpropanoyl) dihydro-2-(3H)-furanone and isopropenyl-4-methyl-1,2-cyclohexanediol had band gap energies of 3.393 eV and 1.588 eV, respectively. However, 5-(3-phenylpropanoyl) dihydro-2-(3H)-furanone may have relatively a large HOMO-LUMO energy gap.



**Table 1.** HOMO-LUMO band gap energies for the selected volatile organic compounds.

Compound	$E_{HOMO}$ (eV)	$E_{LUMO}$ (eV)	$\Delta H = E_{LUMO} - E_{HOMO}$
3,4-dimethyl-3-cyclohexene-1-carbaldehyde	-4.027	-0.109	3.918
5-(3-phenylpropanoyl)dihydro-2-(3H)-furanone	-5.560	-2.167	3.393
4-(2,4-dimethylcyclohexyl)-2-butanone	-4.186	-3.512	0.674
isopropenyl-4-methyl-1,2-cyclohexanediol	-3.451	-1.863	1.588

Evidently, the HOMO-LUMO band-gap for 4-(2,4-dimethylcyclohexyl)-2-butanone is clearly low and therefore could be reactive especially towards biological structures contrary to the fact that ketones are known to be least reactive compared to alcohols and aldehydes. Generally, the band-gap between the HOMO and the LUMO is directly related to the electronic stability of the chemical species [13]. This suggests that 5-(3-phenylpropanoyl)dihydro-2(3H)-furanone having a lower HOMO energy value of -5.560 eV is much more stable making it a good nucleophile compared to 4-(2,4-Dimethylcyclohexyl)-2-butanone which are energetically higher in the LUMO. **Figure 5** and **Figure 6** report the band gap energies for 4-(2,4-dimethylcyclohexyl)-2-butanone and 5-(3-phenylpropanoyl)dihydro-2-(3H)-furanone, respectively.

The key idea of the frontier molecular orbitals theory rests on the fact that most chemical reactions are dominated by the interaction between these frontier orbitals in an electron donor-acceptor regime. The energy gap between the HOMO-LUMO energy levels is a useful parameter of describing and understanding the reactivity of molecules or compounds.

### 3.3. Electron Density Contour Maps

Electron density contour maps provide an understanding of the charge distributions on molecules. Electron density maps were done for 3, 4-dimethyl-3-cyclohexene-1-carbaldehyde, 5-(3-phenylpropanoyl)dihydro-2(3H)-furanone, and isopropenyl-4-methyl-1,2-cyclohexanediol as presented in appendices A, B and C. These Figures are critical in determining regions of high electron density within a molecule. Electron distribution gives insight on the behaviour of particular molecules in understanding the nucleophilic and electrophilic sites in molecular structures. **Figure 7** and **Figure 8** give the 2-D and 3-D electron density maps for 5-(3-phenylpropanoyl)dihydro-2(3H)-furanone as obtained from Chemissian and Gaussian computational platforms, respectively. Regions of low potential are electron rich compared to other regions in the molecule. Evidently, oxygen atoms in 5-(3-phenylpropanoyl)dihydro-2(3H)-furanone 2-D electron density map has a higher electronegativity value than other atoms (C & H) in the structure. Thus, it has a higher charge density around it compared to other atoms. This is clearly shown by deep red coloration in the 3-D structure (**Figure 8**).

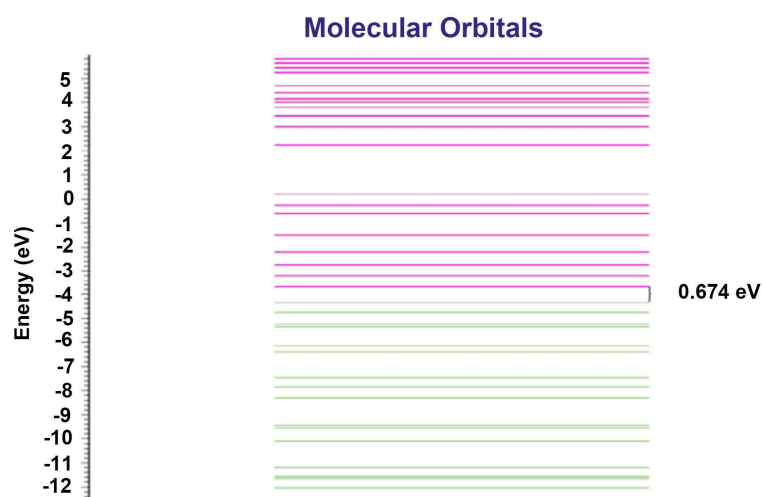


**Figure 5.** The HOMO-LUMO band gap for 4-(2,4-dimethylcyclohexyl)-2-butanone determined using Chemissian.

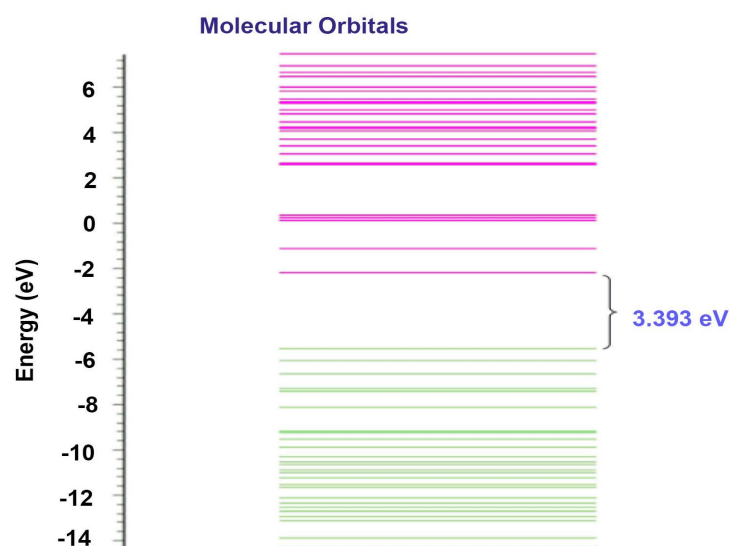


**Figure 6.** The HOMO-LUMO band gap for 5-(3-phenylpropanoyl)dihydro-2-(3H)-furanone determined using Chemissian.

Conservatively, the negative potential sites (red colour) represents regions of electrophilic reactivity and interactions through  $\pi$ - $\pi$  bonding within the aromatic systems and positive potential sites (green colour) represents regions of nucleophilic reactivity [14] **Figure 8**, *vide supra*.

### 3.4. Mechanistic Degradation of 5-(3-Phenylpropanoyl)Dihydro-2(3H)-Furanone

Mechanistic channels attempt to show how starting materials are converted into products during chemical reactions. Thermal decomposition of fuels leads to emission of numerous particulate matter of various classifications that are of public health interest. These compounds include long chain hydrocarbons,



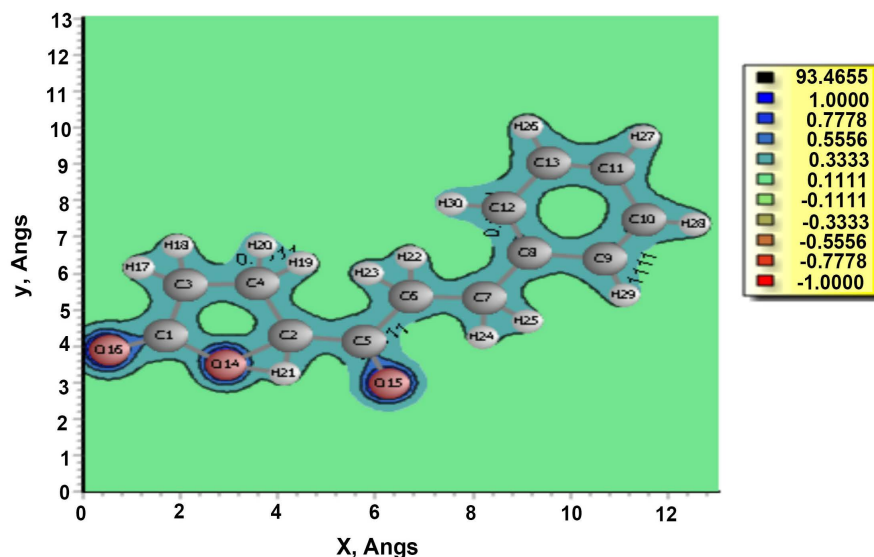


**Figure 7.** 2-D electron density map for 5-(3-Phenylpropanoyl)dihydro-2(3H)-furanone.

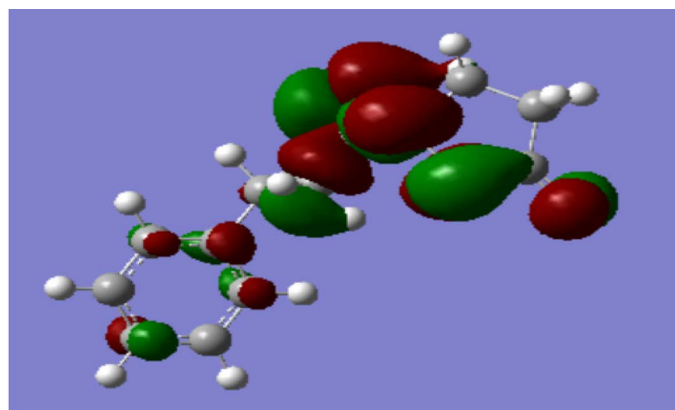


**Figure 8.** 3-D electron density map for 5-(3-phenylpropanoyl)dihydro-2(3H)-furanone at an iso-value of 0.020.

oxygenated by-products, aromatic hydrocarbons among other eco-toxic organics [6]. This study has also proposed the mechanistic formation of free radicals from selected oxygenated by-products, which are noted to be precursors of cancer, general respiratory human health and reactive oxidative stress (ROS) well known for their central role in initiating both physiological and pathophysiological signal transduction [15]. Free radicals are generated from both endogenous and exogenous sources and are known to penetrate the body where they are degraded or metabolized and harmful free radicals are generated as by-products [16]. To investigate the energetics of the selected molecular emissions, Gaussian '16 software employing the B3LYP correlation function and 6-31G basis sets at DFT level of theory were conducted.

Environmental pollutants blamed for a number of illnesses arise as unwanted by-products in various processes, especially in uncontrolled combustion events such as accidental fires, combustion of transport fuels, cigarette smoking and

municipals waste incineration [17]. The major areas of concern focus on the mechanistic formation of environmentally free radicals and their associated impact on human health [18], from chronic respiratory and cardiopulmonary dysfunction as a consequence of oxidative stress induced by reactive oxygen species (ROS) [8].

Clearly, the thermal degradation is predicted to occur via an endothermic energy barriers, **Scheme 1** (routes i and iv). Formational of radicals via route (i) proceeds with an energy of 415.71 kJ/mol considered less important to biological systems [19]. The scission of -C-C-bond in route (iv) for the formation of ethylbenzyl radical and 5-oxotetrahydrofuran-2-carbaldehydyl radical occurs with an enthalpy change of 372.31 kJ/mol which is thermodynamically feasible. Interestingly, route (viii) shows a highly exothermic reaction, with bond dissociation energy of -1250.75 kJ/mol. The conversion of free radicals to their corresponding free molecules occurs through exothermic channels, routes (iii) and (v-ix), scheme 1, vide supra.

Density functional theory calculations have been found to be successful in giving theoretical insights into the reactivity of organic compounds. They provide possible reaction pathways which organic compounds can undergo without necessarily carrying out experimental work which may be both tedious and time consuming. Moreover, computational calculations compliment experimental data. Interestingly, the difference in energy changes between experimental and theoretical work is minimal, and in some cases, computational data has been found to be more accurate than experimental data [20]. Consequently, the energy data reported in this work were derived entirely from computational modeling based on the main objective of this study. There is, however; no known experimental data presented anywhere in literature on this work to necessitate comparative analysis.

#### 4. Conclusion

This study has demonstrated that the thermal decomposition of fuel components of *Croton megalocarpus* biodiesel proceeds chiefly via endothermic energy barriers to form various radicals which may recombine to form free stable molecules proposed to be toxic to humans and the natural environment. Such toxic molecular products may include ketones aldehydes, benzene and its derivatives, among other harmful compounds. The

5-(3-phenylpropanoyl) dihydro-2(3H)-furanone is more electronegative since it has three oxygen atoms compared to other molecules considered in this study which are more electron withdrawing atoms compared to C and H in the structure. Overall, it can be concluded that

5-(3-Phenylpropanoyl) dihydro-2-(3H)-furanone has more electrophilic reactive sites than 4-(2,4-Dimethylcyclohexyl)-2-butanone, 3,4-dimethyl-3-cyclohexene-1-carbaldehyde and isopropenyl-4-methyl-1,2-cyclohexanediol. This observation is supported by the electron density maps reported in this study.

## Acknowledgements

The authors wish to thank the University of KwaZulu-Natal (UKZN), for according JK the opportunity to conduct GC-MS.

## Conflicts of Interest

The authors declare that they have no competing interests regarding the publication of this article.

## References

- [1] Ojirika, E.C., Joel, O.F. and Ugbebor, N.J. (2019) Evaluation of Quality of Automotive Gas Oil Produced by Artisanal Petroleum Refineries in Rivers State, Niger Delta. *SPE Nigeria Annual International Conference and Exhibition*, Society of Petroleum Engineers. <https://doi.org/10.2118/198794-MS>
- [2] Cheruiyot, N.K., Hou, W.C., Wang, L.C. and Chen, C.Y. (2019) The Impact of Low to High Waste Cooking Oil-Based Biodiesel Blends on Toxic Organic Pollutant Emissions from Heavy-Duty Diesel Engines. *Chemosphere*, **235**, 726-733. <https://doi.org/10.1016/j.chemosphere.2019.06.233>
- [3] Chen, S.J., Tsai, J.H., Chang-Chien, G.P., Huang, K.L., Wang, L.C., Lin, W.Y. and Yeh, C.K.J. (2017) Emission Factors and Congener-Specific Characterization of PCDD/Fs, PCBs, PBDD/Fs and PBDEs from an Off-Road Diesel Engine Using Waste Cooking Oil-Based Biodiesel Blends. *Journal of Hazardous Materials*, **339**, 274-280. <https://doi.org/10.1016/j.jhazmat.2017.06.045>
- [4] Yahagi, S.S., Roveda, A.C., Sobral, A.T., Oliveira, I.P., Caires, A.R., Gomes, R.S. and Trindade, M.A. (2019) An Analytical Evaluation of the Synergistic Effect on Biodiesel Oxidation Stability Promoted by Binary and Ternary Blends Containing Multifunctional Additives. *International Journal of Analytical Chemistry*, **2019**, Article ID: 6467183. <https://doi.org/10.1155/2019/6467183>
- [5] Altarawneh, M. and Dlugogorski, B.Z. (2015) Formation of Dibenzofuran, Dibenzop-Dioxin and Their Hydroxylated Derivatives from Catechol. *Physical Chemistry Chemical Physics*, **17**, 1822-1830. <https://doi.org/10.1039/C4CP04168B>
- [6] Mumtaz, M.W., Adnan, A., Mahmood, Z., Mukhtar, H., Malik, M.F., Qureshi, F.A. and Raza, A. (2012) Biodiesel from Waste Cooking Oil: Optimization of Production and Monitoring of Exhaust Emission Levels from Its Combustion in a Diesel Engine. *International Journal of Green Energy*, **9**, 685-701. <https://doi.org/10.1080/15435075.2011.625583>
- [7] Cordeiro, R.S., Vaz, I.C., Magalhaes, S. and Barbosa, F.A. (2017) Effects of Nutritional Conditions on Lipid Production by Cyanobacteria. *Anais da Academia Brasileira de Ciências*, **89**, 2021-2031. <https://doi.org/10.1590/0001-3765201720150707>
- [8] Chendynski, L.T., Mantovani, A.C.G., Savada, F.Y., Messias, G.B., Santana, V.T., Salviato, A. and Borsato, D. (2019) Analysis of the Formation of Radicals in Biodiesel in Contact with Copper and Metallic Alloys via Electronic Paramagnetic Resonance (EPR). *Fuel*, **242**, 316-322. <https://doi.org/10.1016/j.fuel.2019.01.058>
- [9] Assaf, N.W., Altarawneh, M., Oluwoye, I., Radny, M., Lomnicki, S.M. and Dlugogorski, B.Z. (2016) Formation of Environmentally Persistent Free Radicals on  $\alpha$ -Al<sub>2</sub>O<sub>3</sub>. *Environmental Science and Technology*, **50**, 11094-11102. <https://doi.org/10.1021/acs.est.6b02601>
- [10] Frisch, M., Trucks, G., Schlegel, H., Scuseria, G., Robb, M., Cheeseman, J., Scalmani,

- G., Barone, V., Petersson, G. and Nakatsuji, H. (2016) Gaussian 16. Revision A, 3.
- [11] Skripnikov, L. (2016) Chemissian Version 4.43, Visualization Computer Program. <http://www.chemissian.com>
- [12] Ochterski, J.W. (2015) Thermochemistry in Gaussian. Gaussian Inc., Pittsburgh, 1-17. <http://www.gaussian.com>
- [13] Frisch, M., Trucks, G., Schlegel, H., Scuseria, G., Robb, M.A. and Cheeseman, J. (2009) Gaussian 09, Revision B01. Gaussian Inc., Wallingford. <http://www.gaussian.com>
- [14] Hanulikova, B. (2016) Effect of Backbone Conformation and Its Defects on Electronic Properties and Assessment of the Stabilizing Role of  $\pi$ - $\pi$  Interactions in Aryl Substituted Polysilylenes Studied by DFT on Deca[methyl(phenyl)silylene]s. *Chemistry Central Journal*, **10**, 28. <https://doi.org/10.1186/s13065-016-0173-0>
- [15] Forrester, S.J., Kikuchi, D.S., Hernandez, M.S., Xu, Q. and Griendling, K.K. (2018) Reactive Oxygen Species in Metabolic and Inflammatory Signaling. *Circulation Research*, **122**, 877-902. <https://doi.org/10.1161/CIRCRESAHA.117.311401>
- [16] Pizzino, G., Irrera, N., Cucinotta, M., Pallio, G., Mannino, F., Arcoraci, V. and Bitto, A. (2017) Oxidative Stress: Harms and Benefits for Human Health. *Oxidative Medicine and Cellular Longevity*, **2017**, Article ID 8416763. <https://doi.org/10.1155/2017/8416763>
- [17] Mosallanejad, S., Dlugogorski, B.Z., Kennedy, E.M., Stockenhuber, M., Lomnicki, S.M., Assaf, N.W. and Altarawneh, M. (2016) Formation of PCDD/Fs in Oxidation of 2-Chlorophenol on Neat Silica Surface. *Environmental Science and Technology*, **50**, 1412-1418. <https://doi.org/10.1021/acs.est.5b04287>
- [18] Nel, A. (2005) Air Pollution-Related Illness: Effects of Particles. *Science*, **308**, 804. <https://doi.org/10.1126/science.1108752>
- [19] Kibet, J.K. (2016) Computational Modeling of 2-Monochlorophenol and 2-Monochlorothiophenol. *Kabarak Journal of Research and Innovation*, **4**, 49-61.
- [20] Osorio, E., Vasquez, A., Florez, E., Mondragon, F., Donald, K.J. and Tiznado, W. (2013) Theoretical Design of Stable Small Aluminium-Magnesium Binary Clusters. *Physical Chemistry Chemical Physics*, **16**, 2222-2229. <https://doi.org/10.1039/C2CP42015E>